

Simulation of Carrier Transport in Carbon Nanotube Field Effect Transistors

Enzo Ungersböck*, Andreas Gehring*, Hans Kosina*, Siegfried Selberherr*,
Byoung-Ho Cheong[°], and Won Bong Choi[†]

**Institute for Microelectronics, TU Vienna, A-1040 Vienna, Austria*

[°]*Computational Science Engineering Center, SAIT, Suwon 440-600, Korea*

[†]*Materials and Device Laboratory, SAIT, Suwon 440-600, Korea*

Ungersboeck@iue.tuwien.ac.at

Abstract

We discuss models to describe carrier transport in axial and lateral type carbon nanotube field-effect transistors (CNT-FET). Operation is controlled by the electric field from the gate contact which can lead to strong band bending allowing carriers to tunnel through the interface barrier. We find that the difference between lateral and axial CNT-FETs is that in devices with axially aligned carbon nanotubes tunneling becomes negligible and transport can be modeled by means of thermionic emission. In lateral CNT-FETs tunneling dominates for which we present a model for the transmission coefficient using the WKB method and a non-parabolic dispersion relation. The simulated output and transfer characteristics show reasonable agreement with experimental data for both lateral and axial CNT-FET devices.

1. Introduction

Carbon nanotubes belong to the most promising candidates for future nanoelectronic applications. Experiments and theory have shown that the tubes can either be metals or semiconductors. Their electrical properties can rival, or even exceed, the best metals or semiconductors known. The electrical behavior is a consequence of the electronic band structure which depends on the exact position of the carbon atoms forming the tube. Semiconducting nanotubes can be used as active elements in field-effect transistor (FET) designs. While early devices showed poor device characteristics, improvements were achieved by using thinner dielectric films [1].

Recently models to describe the transport properties of carbon nanotubes have been developed [2, 3]. It was shown that carbon nanotubes act as unconventional Schottky barrier transistors. Transistor action is achieved by varying the contact resistance rather than the channel conductance. Transport through the nanotube is ballistic, so the current predominately depends on energy barriers between the source and drain contacts. Since the shape of this energy barrier and hence the operation of the transistor depends crucially on the device geometry, device simulation becomes necessary to predict device performance.

Simulation studies have shown that the shape of the contact electrodes has a high impact on the Schottky barriers and can be used for device optimization [4]. In this paper we compare two common CNT-FET geometries, namely transistors with laterally and axially aligned carbon nanotubes. While lateral CNT-FETs have shown good performance with high $I_{\text{on}}/I_{\text{off}}$ ratios [5], the manufacturability challenges are still significant. Transistors with axially aligned carbon nanotubes [6] show worse device characteristics while being more suitable for large-scale integration. The considered device structures are presented in Section 2. In Section 3 models are discussed which allow the simulation of CNT-FETs in both the thermionic emission and the tunneling regime. Finally the simulations are compared to measurements of a lateral [3] and axial CNT-FET [6].

2. Device Modeling

The structure of axial and lateral CNT-FET devices is shown in Fig. 1. Lateral CNT-FETs resemble conventional MOSFET structures where the silicon channel is replaced by a single-wall or a highly defective multi-wall carbon nanotube connecting the source and drain contacts [4].

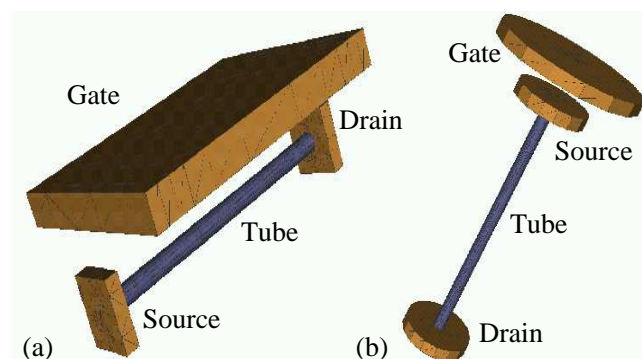


Figure 1. The lateral (a) and axial (b) carbon nanotube device structures

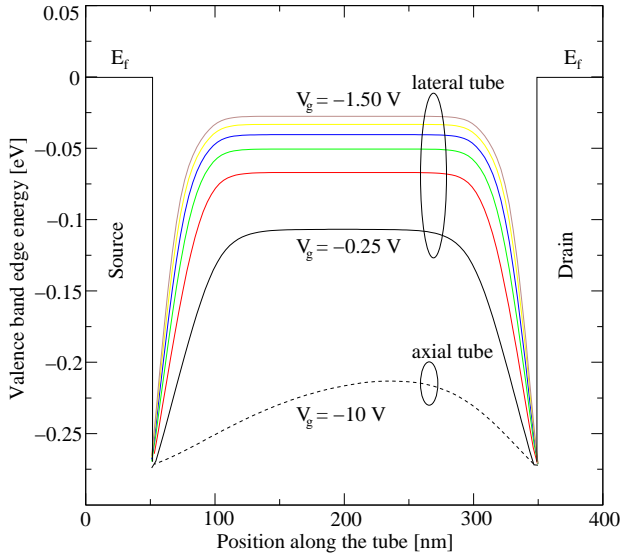


Figure 2. The valence band edge in a lateral CNT-FET at different gate voltages. The dashed line shows the band profile of an axial CNT-FET at $V_g = -10$ V

In axial CNT-FETs the gate contact lies above the drain contact from which it is separated by a thin gate oxide. While this structure has a much smaller footprint as compared to laterally aligned tubes, it has the shortcoming that the capacitive coupling between the gate and the tube is only weak. To get the potential distribution in such devices three-dimensional simulation is required. However, since the principle of carrier transport in carbon nanotubes is still a subject of intense research and for the sake of simplicity we have used the two-dimensional general-purpose device simulator MINIMOS-NT to acquire the potential profile at the surface of the tube.

Since measured characteristics of most CNT-FETs resemble those of conventional p-type FETs the figures concentrate on hole transport and the valence band edge in the nanotube. Still the method is suited for electron transport as well. A band gap of 0.6 eV and undoped tubes have been assumed. The tube is covered in HfO_2 and connected to Al source and drain contacts. Fig. 2 shows the resulting valence band edge along the tube for the lateral and for the axial device at $V_{DS} = 0$ V. In case of lateral CNT-FETs the gate field heavily influences the valence band. Modulating the gate voltage from -0.25 V to -1.5 V, the valence band is shifted upwards towards the Fermi level of the source and drain electrodes. This effectively reduces the energy barrier for holes. At modest gate voltages the carriers have to surmount a large energy barrier. Tunneling current is small and thermionic emission prevails. Increasing the gate voltage leads to a reduction of the energy barrier till tunneling dominates over thermionic emission. The threshold voltage V_{th} of the device can be defined as the gate voltage necessary to shift the valence band up so that the tunneling current exceeds thermionic

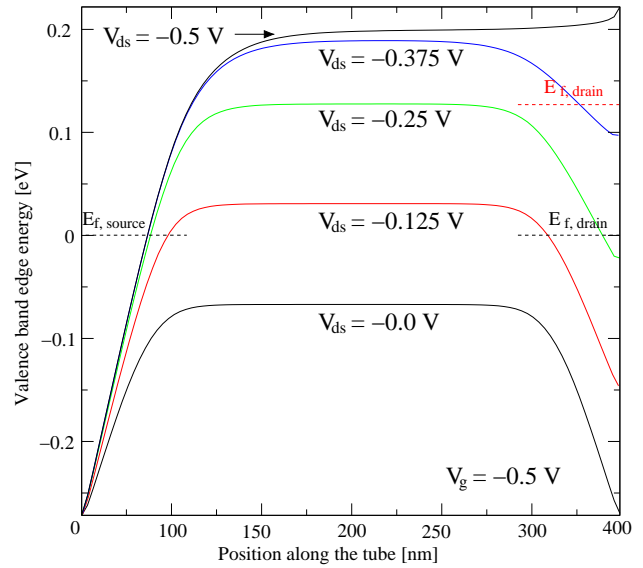


Figure 3. Valence band edge of a lateral CNT-FET for various drain voltages. One can observe suppression of the Schottky barrier at the drain contact

emission. The current saturates as soon as the second barrier is completely suppressed. Hence all electrons that can tunnel through the source barrier will contribute to the current. The axial device, on the other hand, does not exhibit this behavior even for a gate voltage of -10 V.

For a fixed gate voltage the band edge energies also depend on the drain voltage, as shown in Fig. 3 for a gate voltage of $V_g = -0.5$ V. At zero drain voltage the tunneling barrier is strong and thermionic emission dominates over tunneling. When V_{DS} is decreased, the band edge at the drain side moves up and the effective barrier seen by holes coming from the source contact is reduced. This leads to an increase of tunneling current. At drain voltages below -0.375 V the drain tunneling barrier vanishes completely. The source energy barrier is fixed by the potential at the source contact and remains relatively insensitive to an increase of V_{DS} . This gives rise to an output characteristics which is characterized by three distinguishable regions: an exponential region where thermionic emission dominates over tunneling, a linear region where tunneling prevails and the drain barrier decreases, and a saturation regime with a constant current.

For axial devices the gate field is blocked to a large amount by the underlying source contact (see Fig. 2). Even when applying relatively high gate voltages the effect on the barrier between source and drain is weak. The charge carriers have to surmount a potential barrier with two peaks at the contacts which is almost constant throughout the carbon nanotube. In this sense V_{th} is never reached and thermionic emission will at all voltages dominate over tunneling. This results in output characteristics which resemble those of conventional Schottky barrier transistors.

3. Transport Modeling

Modeling of tunneling current is crucial for lateral CNT-FETs, while carrier transport in axial CNT-FETs can be described within the Schottky emission theory.

3.1. Modeling of Tunneling Current

To account for coherent transport in the nanotube the Landauer Büttiker formula has been implemented in MINIMOS-NT. The drain current through the nanotube is given by an integration in the energy domain [7]

$$I_d(V_{ds}) = \frac{4q}{h} \int dE (f_s^0(E) - f_d^0(E)) TC(E), \quad (1)$$

where TC is the transmission coefficient and $f_{d,s}^0$ are the equilibrium Fermi functions at the source and drain contacts. The transport is ballistic, hence the current does neither depend on the length nor on the cross section of the carbon nanotube. The factor 4 in (1) stems from the twofold band and the twofold spin degeneracy.

In carbon nanotubes the dispersion relation cannot be described by a simple parabolic shape. Instead

$$E_{\pm n}(k) = \pm \frac{\sqrt{3}a\gamma_0}{2} \sqrt{\kappa(n)^2 + k^2} \quad (2)$$

has been used to approximate the band structure in the vicinity of the Fermi energy [8]. In this expression a denotes the lattice constant, γ_0 is the transfer integral, and κ_n is related to the radius R of the nanotube via

$$\kappa_n = \frac{1}{R} \left(n - \frac{1}{3} \right). \quad (3)$$

Here, the value n denotes the band index. Accounting for this band structure, the transmission coefficient of carriers from band n can be estimated within the commonly used Wentzel Kramers Brillouin (WKB) approximation:

$$TC_n(E) = \exp \left(-2 \int k(x) dx \right) \quad (4)$$

with the wave number

$$k = \frac{|\kappa_0|}{2} \sqrt{\left(\frac{\kappa_n}{\kappa_0} \right)^2 - \left(\frac{E - V(x)}{E_g/2} \right)^2}. \quad (5)$$

In this expression $V(x)$ is the position dependent band edge along the tube. The band gap E_g of single walled carbon nanotubes is related to the radius, $E_g = 0.9, eV/2R$, where R is given in nm.

Numerical integration is performed only within classical turning points. Note that the WKB method can only be used for slowly varying potentials and has the shortcoming that it fails at the classical turning points ($E = V$). Furthermore, the WKB method does not account for wavefunction interference effects which may occur due to the two separated barriers.

An alternative approach to calculate the transmission coefficient is to solve Schrödinger's equation with open

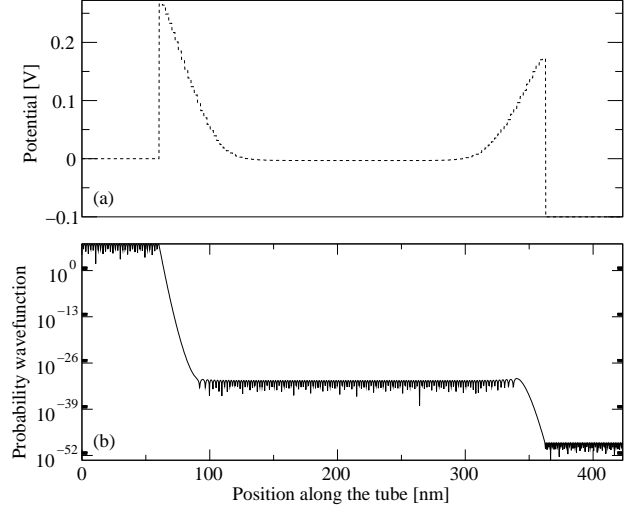


Figure 4. Potential along the nanotube at $V_{ds} = -0.1$ V (a) and the hole probability wavefunction (b)

boundary conditions in the whole nanotube. This has been done using the quantum transmitting boundary method (QTBM) [9]. This method has been preferred over transfer-matrix based schemes due to its better numerical stability. The resulting wavefunction at an energy of 0.1 eV is shown in Fig. 4. Exponential decay occurs in the barrier regions. Although no interference effects have been observed for long nanotubes, these affects can influence shorter devices.

3.2. Modeling of Thermionic Emission

The qualitative band diagram for axial CNT-FETs (see Fig. 2) motivates to describe the current density through the tube as emission over a Schottky barrier. Within the thermionic emission theory the current density can be written as [10]

$$J = C \exp \left(-\frac{q\Phi_B}{k_B T \gamma} \right) \cdot \left[\exp \left(\frac{qV_{DS}}{k_B T \gamma} \right) - 1 \right],$$

where $C = 4\pi m_{\text{eff}} q k_B^2 T^2 / h^3$ and the parameter γ has been introduced to describe the exponential slope of the IV-characteristics. To get a model which only depends on the gate-source and drain-source voltages, the values of Φ_B and γ have been fitted to measurement results with the gate-source voltage as parameter. This compact model has also been implemented in MINIMOS-NT, enabling the simulation of complete circuits.

4. Results and Conclusion

A lateral CNT-FET with a 20 nm HfO_2 layer ($\epsilon_r = 11$) between the gate and the carbon nanotube and a source drain separation of 300 nm has been simulated. The single wall carbon nanotube has a radius of 0.7 nm and a bandgap of 0.6 eV. The subthreshold characteristics of this device for a drain voltage of $V_{DS} = -1.2$ V is shown

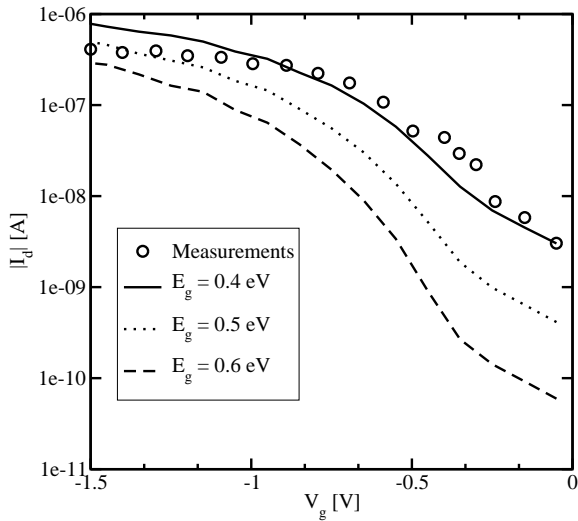


Figure 5. Experimental data and simulation results for a lateral CNT-FET. Increasing the tube radius reduces the band gap and thus decreases the threshold voltage

in Fig. 5. The experimental data [3] show reasonable agreement with the simulation results. The best fit is obtained if the radius of the tube is assumed to be 0.9 nm resulting in a band gap of 0.4 eV. However, we point out that the model has to be enhanced in order to take account for the linear increase of the drain current I_d at high drain voltages of fully turned on devices.

Finally we used the thermionic emission model for the simulation of an axial CNT-FET. The conducting channel of this device is a highly defective multi-wall carbon tube with a diameter of approximately 20 nm, covered by SiO_2 and attached to source and drain contacts. The measured band gap of this device was 0.6 eV. Good agreement to experimental data [6] is found (see Fig. 6). Note that these measurements have been performed at liquid helium temperature. The low magnitude of the resulting drive current and the low $I_{\text{on}}/I_{\text{off}}$ ratio makes the usage of axial devices as a replacement of MOSFET devices questionable.

We showed how transport through carbon-nanotube devices can be understood as tunneling or thermionic emission depending on the device geometry. Lateral CNT-FETs allow good coupling between gate and tube, enabling output characteristics with good $I_{\text{on}}/I_{\text{off}}$ ratios. Axial CNT-FETs can be described assuming thermionic emission. The presented models can be used to describe carrier transport in both types of carbon nanotubes.

5. Acknowledgements

This work was supported by the National Program for Tera-level Nanodevices of the Korea Ministry of Science and Technology as one of the 21st Century Frontier Programs.

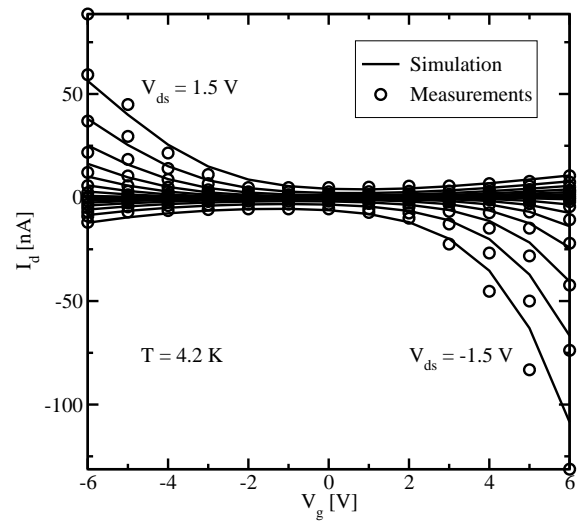


Figure 6. Output characteristics of an axial multi-wall CNT-FET at 4.2K compared to simulations assuming thermionic emission

- [1] S. J. Wind, J. Appenzeller, R. Martel, V. Derycke, and Ph. Avouris, "Vertical Scaling of Carbon Nanotube Field-Effect Transistors Using Top Gate Electrodes," *Appl.Phys.Lett.*, vol. 80, no. 20, pp. 3817–3819, 2002.
- [2] T. Nakanishi, A. Bachtold, and C. Dekker, "Transport Through the Interface between a Semiconducting Carbon Nanotube and a Metal Electrode," *Physical Review B*, vol. 66, no. 073307–1–4, 2002.
- [3] J. Appenzeller, J. Knoch, R. Martel, V. Derycke, S. J. Wind, and P. Avouris, "Carbon Nanotube Electronics," *IEEE Trans. Nanotechnology*, vol. 1, no. 4, pp. 184–189, 2002.
- [4] S. Heinze, J. Tersoff, R. Martel, V. Derycke, J. Appenzeller, and Ph. Avouris, "Carbon Nanotubes as Schottky Barrier Transistors," *Physical Review Letters*, vol. 89, no. 10, pp. 106801–1–4, 2002.
- [5] R. Martel, T. Schmidt, H. R. Shea, T. Hertel, and Ph. Avouris, "Single- and Multi-Wall Carbon Nanotube Field-Effect Transistors," *Appl.Phys.Lett.*, vol. 73, no. 17, pp. 2447–2449, 1998.
- [6] W. B. Choi, J. U. Chu, K. S. Jeong, E. J. Bae, and J. W. Lee, "Ultrahigh-Density Nanotransistors by Using Selectively Grown Vertical Carbon Nanotubes," *Appl.Phys.Lett.*, vol. 79, no. 26, pp. 3696–3698, 2001.
- [7] S. Datta, *Electronic Transport in Mesoscopic Systems*, Cambridge University Press, 1995.
- [8] H. Ajiki and T. Ando, "Electronic States of Carbon Nanotubes," *Journal of the Physical Society of Japan*, vol. 62, no. 4, pp. 1255–1266, 1993.
- [9] W. R. Frensley, "Numerical Evaluation of Resonant States," *Superlattices & Microstructures*, vol. 11, no. 3, 1992.
- [10] E. H. Rhoderick and R. H. Williams, *Metal-Semiconductor Contacts*, Oxford Press, 1988.